Honeycomb Charge Ordering in $IrTe_2$

Hyo Sung Kim,[1,2] Soo-Ran Kim,[2] Kyoo Kim,[2] Byung Il Min,[2]
Yong-Heum Cho,[2,3] Sang-Wook Cheong,[2,3,4] and Han Woong Yeom[1,2,*]

[1] *Center for Artificial Low Dimensional Electronic Systems, Institute for Basic Science (IBS), Pohang 790-784, Korea*
[2] *Department of Physics, Pohang University of Science and Technology, Pohang 790-784, Korea*
[3] *Laboratory for Pohang Emergent Materials, Pohang University of Science and Technology, Pohang 790-784, Korea*
[4] *Rutgers Center for Emergent Materials and Department of Physics and Astronomy, Piscataway, New Jersey 08854, USA*

(Dated: May 5, 2015)

We report on the observation of a unique honeycomb charge ordering of the cleaved $IrTe_2$ surface by high-resolution scanning tunneling microscopy (STM) and spectroscopy (STS). $IrTe_2$ was recently established to exhibit intriguing stripe charge orderings. Here, we show that the stripe charge order coexists with a metastable honeycomb phase formed locally. The atomic and electronic structures of the honeycomb phase are consistent with the stripe phase indicating unambiguously its charge order nature. A simple model of the honeycomb structure is suggested based on the overlap of three degenerate stripe orders, which is analogous to the $3q$ state description of a skyrmion. We suggest that the honeycomb charge order can be a route to an exotic Dirac electron system.

The spatial ordering of charges due to the Coulomb interaction has been one of the key physics in complex electronic systems with exotic emerging quantum states such as high temperature superconductivity in cupurates [1, 2] and colossal magnetoresistance in manganese oxides [3, 4]. Most of long range charge orderings found so far are stripe structures [5] while hexagonal structures are frequently observed for two dimensional (2D) charge density wave (CDW) systems [6–8]. The recent development of microscopy techniques such as scanning tunneling microscopy (STM) has made it possible to disclose atomic scale details of charge orderings in low dimensional systems. One of the important achievements of the microscopic studies is the observation of the checkerboard-type charge orderings in a high temperature superconductor [9] and a manganite perovskite [10, 11]. The origin of the checkerboard order is still not fully understood but it corresponds to the intrinsic or extrinsic overlap of two stripe orders [12].

In this letter, we identify for the first time the honeycomb charge ordering for a recently found charge order material of $IrTe_2$ with STM in coexistence with the stripe phases observed previously. The $IrTe_2$ is currently under extensive investigation due to its unusual characteristics of the charge ordering together with the metallic property. $IrTe_2$ is a layered material and exhibits the charge order (Ir $5d^{3+}$- Ir $5d^{4+}$) transition into stripe phases [$\vec{q}$ =(1/5, 0,–1/5)] with a large hysteresis and a nontrivial remnant metallic conductivity [13–15]. This charge order seems to compete with the superconductivity upon doping electrons, suggesting a quantum critical behavior [16–20]. The driving force of the transition is not fully understood yet but the CDW nature was ruled out [21–23]. The interplay of various different degrees of freedom is widely recognized, such as the strong structural distortions involving the Ir-Ir dimerization and the depolymerization of the Te-Te interlayer bonding, the Ir $5d$ charge disproportionation, the strong reorganization of Fermi surfaces, and the strong spin-orbit coupling.

The honeycomb phase observed here is metastable and compete with the more stable stripe orders. The charge-ordered nature of the honeycomb structure is well supported by its electronic structure revealed by scanning tunneling spectroscopy (STS). The microscopic model of the honeycomb phase is proposed based on the overlap of three rotationally degenerated stripe orderings, which is analogous to the $3q$ state description of a skyrmion and the domain wall ordering of incommensurate CDW systems [7, 24]. This phase has not been noticed in the bulk diffraction measurement and thus the surface origin is likely. The honeycomb charge organization in a 2D system leads readily to a Dirac electron system [25]. With the strong spin-orbit coupling, the honeycomb charge arrangement of Ir $5d$ states may open a route to exotic Dirac electron systems.

The single crystals of $IrTe_2$ were grown by Te flux using pre-sintered $IrTe_2$ polycrystals as reported previously [13]. The sample was cleaved in a vacuum better than 5×10^{-10} torr at room temperature or 86 K, lower than the transition temperature. All the STM measurements were obtained with a commercial ultrahigh vacuum cryogenic STM (Specs, Germany) in the constant-current mode with PtIr tips at 78 K and 1.1 K. The differential conductance, dI/dV, was measured using the lock-in detection with a modulation of 1 kHz. For the total energy calculation, we constructed a $6\times6\times1$ supercell consisting of monolayers separated by vacuum distance about 2.0 nm and employed the density functional theory band calculation as implemented in the pseudopotential plane wave package, VASP [26, 27]. For the exchange-correlation functional, the generalized gradient approximation in PBEsol scheme has been used [28]. The spin-orbit effect was included.

Figure 1(a) shows a cleaved $IrTe_2$ surface where a Te

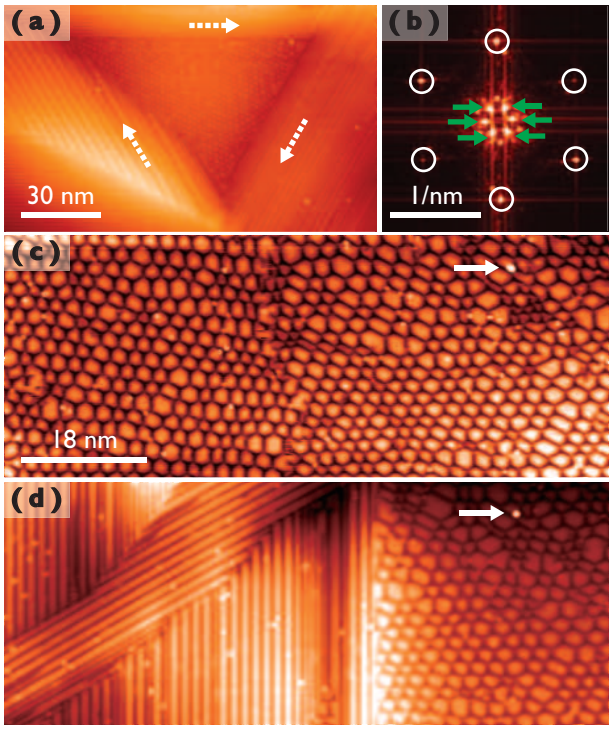

FIG. 1. (color online) STM topographies of the cleaved $IrTe_2$ at 78 K. (a) A typical cleaved $IrTe_2$ surface shows honeycomb and stripe phases coexisting. (b) The FFT image of the honeycomb phase domain shown in (c). White circles and green arrows indicate the periodicities of the hexagons and atoms (2.5 nm and 0.393 nm, respectively). (d) The topography obtained at the same position as (c) after a time interval of 13 min, showing the irreversible transition into the stripe phase. White arrows indicate the defect, used as the position reference mark. Tunneling parameters are $V_s = 1$ V, $I_t = 0.1$ nA

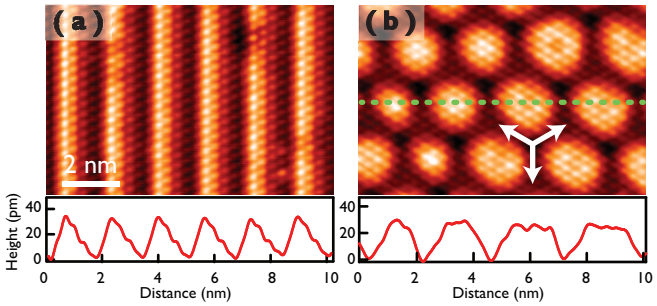

FIG. 2. (color online) Atom-resolved STM topographies of (a) the ×5 stripe phase as well as (b) the honeycomb structure taken at near the Fermi energy ($V_s = 20$ mV). STM line profiles crossing the stripes and hexagons [along the dashed line in (b)] are also given. The white arrows indicate the crystalline direction of $IrTe_2$.

layer is exposed [29–31]. As reported previously, various stripe phases with three different orientations (arrows in the figure) and with different spacings of ×3, ×5, ×8, and ×11 are observed as inhomogeneous mixtures [14, 15]. We previously established that the cascade of stripe phases are based on the building block structures of ×3 and ×5 [Fig. 2(a)] [32]. In addition to the stripe phases, we find that the surface below the transition temperature exhibits another distinct phase with a hexagonal symmetry as enclosed with stripe phases of three different orientations. Figure 1(c) shows one such domain, which is composed of hexagons and honeycomb wall lattice of between 5 (1.7 nm) and 8 times (2.7 nm) the lattice constant [29, 30]. The Fourier transformation of the STM image [Fig. 1(b)] indicates that these hexagons have a quasi long range order with a rather well defined average periodicity of 2.5 nm. The areal ratio between the stripe and honeycomb phases depends on different samples, different cleavages and on different parts of the surface but we always find non-negligible portion of it on the surface [33]. A large domain of the honeycomb phase can extend to a few hundred nm, which is readily formed by the rapid cooling of the sample from room temperature. However, the honeycomb phase is not fully stable. Very rarely but the honeycomb phase spontaneously converts to the stripe phase as shown in Figs. 1(c) and 1(d). At very low temperature of 1 K, the strong tunneling current pulse (in the filled state at a large bias than 0.3 V) can convert the honeycomb phase into the stripes or vice versa [33]. Otherwise, the honeycomb domains formed are very stable. These observations indicate that the honeycomb phase is a metastable phase whose energy is but keen to that of the stripe phases through a large energy barrier.

Figure 2 shows detailed atomic scale structures of the stripe and the honeycomb phase. The stripe phase exhibits rows of atoms with the periodically modulated contrast, which was shown to be bias-independent and well characterized as due mainly to the vertical structural modulation of the Te surface layer [32, 33]. The Te rows with the bright contrasts are buckled up due to the dimerization of Ir rows underneath [21, 22]. Note that there exist three dark rows and two bright ones in the most widely found stripe phase of the ×5 periodicity, underneath which the Ir atomic rows of $5d^{3+}$ and $5d^{4+}$ states are located, respectively. In contrast, the honeycomb phase shows quasi regular hexagons of the bright contrast as surround by honeycomb wall lattice of the dark contrast. However, we note that the dark and bright contrast are consistent in the tunneling current [the apparent height in the corresponding line profiles of Figs. 2(c)] in both phases [33]. That is, it is rather straightforward that the honeycomb structure consists of similar structural motifs, the Te buckling and ir dimers, to the stripe phase.

The similarity of the stripe and the honeycomb phase is not limited to the atomic structure represented by the topographic contrast. Figure 3(a) shows the STS spectra taken for the bright and dark atomic rows of the

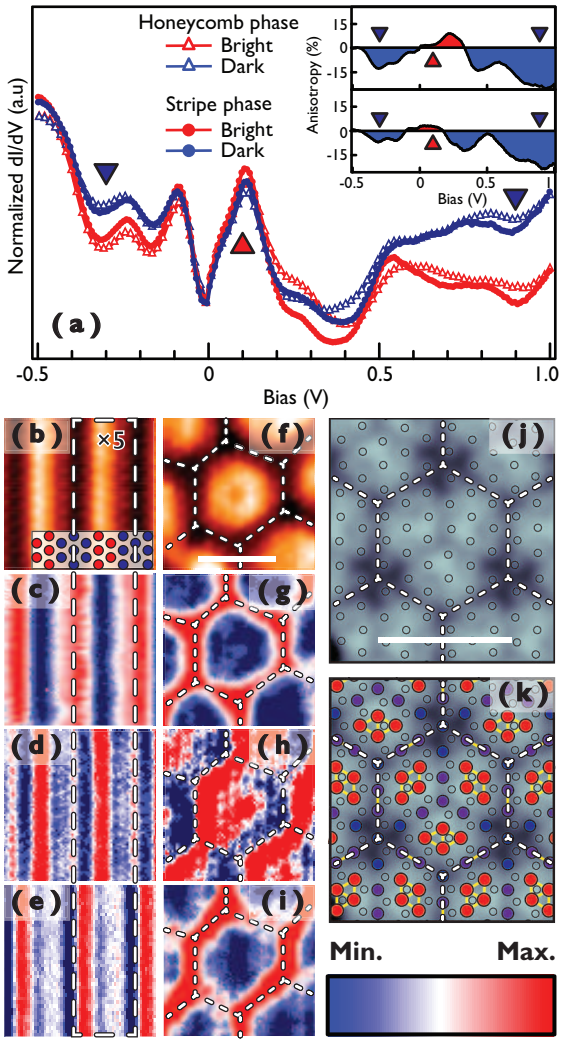

FIG. 3. (a) Averaged STS (dI/dV) spectra from bright and dark regions of both the honeycomb and the stripe phases. (b) A STM topography (V_s = 20 mV) of the stripe phase and (c), (d) and (e) spatially resolved dI/dV maps (V_s = -0.3 V, 0.1 V and +0.9 V, respectively) measured simultaneously. The corresponding (f) STM topography and (g), (h) and (i) the dI/dV maps of the honeycomb phase. White dashed line indicates the single ×5 stripe and a hexagon. (j) The height profile of the Te surface atoms (circles) of the monolayer hexagonal structure shown in (k), where the underlying Ir atoms of 4+ (red), 3+ (or less charged than 4+) (blue) states are also shown. The dimerized Ir atoms are connected by yellow rods. The 2 nm scale bar is shown in (f) and (j).

stripe and the honeycomb phase. These spectra are almost identical, indicating that the electronic structures of these two phases are almost the same. The prominent peak and dip structures in the energy range shown is thought to be due to the Te depolymerization or dimerization, which is intimately entangled with the Ir charge ordering and dimerization [21, 22, 31]. The charge ordering is represented by the spectral intensity reduction in both filled and empty states (-0.5 – 0 and 0.3 – 1.0 V) on the Te rows with a bright contrast in the STM image. The consistent electronic structure of the stripe and the honeycomb phase can further be confirmed by dI/dV maps [Figs. 3(b) – (i)], which reveal the atomic scale lateral variation of the local density of states (LDOS) in the surface Te layer. As detailed previously [32], in the stripe phase, the LDOS at +0.1 (-0.3 and +0.9) eV is enhanced at the bright (dark) atomic rows of the topography [33]. This directly shows the charge ordering in the Te layer, which is coupled with that of the Ir layer underneath. This LDOS modulation is copied in the honeycomb phase as apparently shown in the figure although there is extra symmetry breaking in the hexagonal phase, the inequivalent LDOS intensity for the certain parts of the hexagon [Figs. 3(h) and 3(i)]. We thus can conclude that the stripe and the honeycomb phase have very similar atomic and electronic structure. This means that the bright hexagon in the STM image of the honeycomb phase is composed of protruded Te atoms with the dimerized Ir $5d^{4+}$ atoms underneath and the dark honeycomb walls of Te atoms bonded to Ir $5d^{3+}$ atoms.

The present honeycomb phase is unique among charge order materials while it can be compared with the checkerboard charge ordering for two fold symmetric crystals [9, 12]. In the case of CDW, domain walls of incommensurate orderings exhibit the competition between the stripe and the hexagonal honeycomb phase [6–8, 34]. Such a competition is in fact a general phenomenon for incommensurate superstructures, where their relative stability is determinded by the sign of the domain wall crossing energy. The uniqueness of the present system is that the present stripe orders are commensurate ones and is not a CDW system and not even insulating.

The above similarity between the present system and the 2D incommensurate phases suggests that the honeycomb phase may be a 2D ordering in contrast to the strong interlayer coupling of the stripe phases [37]. In supporting this, the previous x-ray diffraction study did not notice this hexagonal order [13, 31]. A different ordering is highly likely on the surface, especially though the different amount of total charges on the surface layer, the weakening of the Te-Te interlayer bonding, and the possible surface strain.

Based on the above results, we try to construct the structure model of the honeycomb phase from that of the stripe phase. As shown in Figs. 3(b), the stripe phase is composed of three dark contrast rows (blue atoms) and two bright ones (red), under which Ir^{3+} and Ir^{4+} rows exist, respectively [21, 22]. Since there exist three rotationally degenerate ×5 stripes, we can simply overlap these three structures. This idea is consistent with the fact the the hexagonal phase domain is always enclosed with stripe phases with three different orientations. This overlap obviously yields the hexagonal unit cell with the dark trenches as the hexagonal walls. Within this model, one

can understand the varying size of the hexagons based on the coexistence and competition of the $\times 3$, $\times 5$ and $\times 8$ stripe orders. The feasibility of the present model is checked by the first principles total energy calculation using a relatively small unit cell of $6\times6\times1$. We found that the hexagonal structure is not stabilized in the bulk configuration but can be stabilized for the monolayer under the compressive strain of about 10 percent. The fully relaxed structure is shown in Fig. 3(k), where the hexagon is composed of eighteen Ir dimers (yellow rods). As suggested above, hexagon and the honeycomb wall network are mainly composed of Ir^{4+} and Ir^{3+} (or less charged than 4+) atoms, respectively. This hexagon corresponds to one of the smallest hexagons observed. The height distribution of the Te surface atoms in this structure is shown in Fig. 3(j), which is qualitatively consistent with the STM topography of Fig. 3(f). Further refinements of the model is obviously required since the LDOS maps of Fig. 3(g) indicates a much higher degree of honeycomb charge ordering than the present calculation and there is an extra symmetry breaking of the hexagon in the LDOS maps. Howeverm we suggest that this model is a reasonable starting point, which strongly indicates the charge order, two-dimensional and strain origin of the hexagonal phase.

The essence of the present model, the microscopic overlap of the three rotated charge order q, is similar to the $3q$ model of the skyrmion in the 2D triangular spin system [24]. The stabilization of the $3q$ state is basically a nonlinear effect due to the higher order term in the Landau-Ginzburg Free energy. Consistent to the present picture, the local-strain-induced stripe phase was recently reported for $NbSe_2$ with the host hexagonal CDW ordering [36]. Combined with the present finding, this indicates that the competition between $1q$ and $3q$ state is general, irrespective of the detailed mechanism and energetics of charge orderings.

Very recently, the STM study of the doped samples with a superconduction ground state disclosed a disordered honeycomb phases very similar to the present one [39]. We also confirmed this with our own doped samples. The occurrence of the honeycomb phase on the doped samples can be understood by the strain or the reduced interlayer coupling induced by dopants. This observation indicates the importance of the honeycomb charge order for the intriguing fundamental properties of $IrTe_2$. We can further comment that the honeycomb ordering of charge in principle indicates the formation of a Dirac electron system as recently demonstrated for the honeycomb manipulation of the surface state of Cu(111) [25]. The realization of such an artificial Dirac electronic system is under investigation currently. What is very much interesting in the present system is that such a Dirac electron system formed along the present honeycomb wall lattice can be very much exotic due to the strong spin-orbit interaction of the Ir $5d$ electrons leading to a quantum spin Hall system [38].

In summary, we find a metastable honeycomb broken symmetry phase on the surface of $IrTe_2$ at low temperature with STM and STS. The honeycomb phase coexists with the stripe charge order phases identified previously. The structural and electronic properties of the stripe and the honeycomb phases are almost identical revealing the charge order nature of the honeycomb phase too. A preliminary two dimensional model of the honeycomb phase is suggested based on the idea of the overlap of the three rotationally degenerate stripe phases. The further investigation of the honeycomb charge order would be highly interesting in creating an artificial Dirac electron system with a strong spin-orbit coupling.

This work is supported by Institute for Basic Science (Grant No. IBS-R014-D1). YHC and SWC are partially supported by the Max Planck POSTECH/KOREA Research Initiative Program (Grant No. 2011-0031558) through NRF of Korea funded by MEST. We acknowledge Tae-Hwan Kim for the technical help of in STM measurements and Ki-Seok Kim for enlightening discussion.

* yeom@postech.ac.kr

[1] M. I. Salkola, V. J. Emery, and S. A. Kivelson, Phys. Rev. Lett. **77,** 155 (1996).
[2] J. M. Tranquada, B. J. Sternlieb, J. D. Axe, Y. Nakamura, and S. Uchida, Nature **375,** 561 (1995).
[3] R. von Helmolt, J. Wecker, B. Holzapfel, L. Schultz, and K. Samwer, Phys. Rev. Lett. **71,** 2331 (1993).
[4] S. Jin, T. H. Tiefel, M. McCormack, R. A. Fastnacht, R. Ramesh, and L. H. Chen, Science **264,** 413 (1994).
[5] C. Renner, G. Aeppli, B.-G. Kim, Y.-A. Soh, and S.-W. Cheong, Nature **416,** 518 (2002).
[6] R. M. Fleming, D. E. Moncton, D. B. McWhan, and F. J. DiSalvo, Phys. Rev. Lett. **45,** 576 (1980).
[7] P. Bak, D. Mukamel, J. Villain, and K. Wentowska, Phys. Rev. B **19,** 1610 (1979).
[8] P. Bak and D. Mukamel, Phys. Rev. B **19,** 1604 (1979).
[9] M. Vershinin, S. Misra, S. Ono, Y. Abe, Y. Ando, and A. Yazdani, Science **303,** 1995 (2004).
[10] P. G. Radaelli, D. E. Cox, M. Marezio, and S.-W. Cheong, Phys. Rev. B **55,** 3015 (1997).
[11] S. Mori, C. H. Chen, and S.-W. Cheong, Nature **392,** 473 (1998).
[12] J. A. Robertson, S. A. Kivelson, E. Fradkin, A. C. Fang, and A. Kapitulnik, Phys. Rev. B **74,** 134507 (2006).
[13] J. J. Yang, Y. J. Choi, Y. S. Oh, A. Hogan, Y. Horibe, K. Kim, B. I. Min, and S.-W. Cheong, Phys. Rev. Lett. **108,** 116402 (2012).
[14] P.-J. Hsu, T. Mauerer, M. Vogt, J. Yang, Y. S. Oh, S.-W. Cheong, M. Bode, and W. Wu, Phys. Rev. Lett. **111,** 266401 (2013).
[15] T. Machida, Y. Fujisawa, K. Igarashi, A. Kaneko, S. Ooi, T. Mochiku, M. Tachiki, K. Komori, K. Hirata, and H. Sakata, Phys. Rev. B **88,** 245125 (2013).
[16] M. Kamitani, M. S. Bahramy, R. Arita, S. Seki, T.

Arima, Y. Tokura, and S. Ishiwata, Phys. Rev. B **87,** 180501 (2013).
[17] J. Guo, Y. Qi, and H. Hosono, Phys. Rev. B **87,** 224504 (2013).
[18] H. Lei, K. Wang, M. Abeykoon, E. Bozin, J. B. Warren, and C. Petrovic, arXiv:1307.7029.
[19] A. Kiswandhi, J. S. Brooks, H. B. Cao, J. Q. Yan, D. Mandrus, Z. Jiang, and H. D. Zhou, Phys. Rev. B **87,** 121107 (2013).
[20] D. J. Yu, F. Yang, L. Miao, C. Q. Han, M.-Y. Yao, F. Zhu, Y. R. Song, K. F. Zhang, J. F. Ge, X. Yao, Z. Q. Zou, Z. J. Li, B. F. Gao, C. Liu, D. D. Guan, C. L. Gao, D. Qian, and J.-f. Jia, Phys. Rev. B **89,** 100501 (2014).
[21] G. Pascut, K. Haule, M. Gutmann, S. Barnett, A. Bombardi, S. Artyukhin, T. Birol, D. Vanderbilt, J. Yang, S.-W. Cheong, and V. Kiryukhin, Phys. Rev. Lett. **112,** 086402 (2014).
[22] H. Cao, B. C. Chakoumakos, X. Chen, J. Yan, M. A. McGuire, H. Yang, R. Custelcean, H. Zhou, D. J. Singh, and D. Mandrus, Phys. Rev. B **88,** 115122 (2013).
[23] B. Joseph, M. Bendele, L. Simonelli, L. Maugeri, S. Pyon, K. Kudo, M. Nohara, T. Mizokawa, and N. L. Saini, Phys. Rev. B **88,** 224109 (2013).
[24] X. Z. Yu, Y. Onose, N. Kanazawa, J. H. Park, J. H. Han, Y. Matsui, N. Nagaosa, and Y. Tokura, Nature **465,** 901 (2010).
[25] K. K. Gomes, W. Mar, W. Ko, F. Guinea, and H. C. Manoharan, Nature **483,** 306 (2012).
[26] G. Kresse and J. Furthmuller, Comput. Mater. Sci. **6,** 15 (1996).
[27] G. Kresse and J. Furthmuller, Phys. Rev. B **54,** 11169 (1996).
[28] J. P. Perdew, A. Ruzsinszky, G. I. Csonka, O. A. Vydrov, G. E. Scuseria, L. A. Constantin, X. Zhou, and K. Burke, Phys. Rev. Lett. **100,** 136406 (2008).
[29] S. Jobic, R. Brec, and J. Rouxel, J. Alloys Compd. **178,** 253 (1992).
[30] S. Jobic, R. Brec, and J. Rouxel, J. Solid State Chem. **96,** 169 (1992).
[31] Y. S. Oh, J. J. Yang, Y. Horibe, and S.-W. Cheong, Phys. Rev. Lett. **110,** 127209 (2013).
[32] H. S. Kim, T.-H. Kim, J. J. Yang, S.-W. Cheong, and H. W. Yeom (to be published)
[33] See Supplemental Material at http://link for the formation condition of the hexagonal phase and its detailed electronic structure.
[34] T. Garel and S. Doniach, Phys. Rev. B **26,** 325 (1982).
[35] D. B. McWhan, J. D. Axe, and R. Youngblood, Phys. Rev. B **24,** 5391 (1981).
[36] A. Soumyanarayanan, M. M. Yee, Y. He, J. v. Wezel, D. J. Rahn, K. Rossnagel, E. W. Hudson, M. R. Norman, and J. E. Hoffman, Proc. Natl. Acad. Sci. U.S.A. **110,** 1623 (2013).
[37] P. W. Forsbergh, Phys. Rev. **76,** 1187 (1949).
[38] K.-H. Jin and S.-H. Jhi, Phys. Rev. B **87,** 075442 (2013).
[39] Y. Fujisawa, T. Machida, K. Igarashi, A. Kaneko, T. Mochiku, S. Ooi, M. Tachiki, K. Komori, K. Hirata, H. Sakata, arXiv:1503.00898.